Polymer Bulletin
https://doi.org/10.1007/s00289-018-2645-y

ORIGINAL PAPER

Structural, electrical and ion transport properties of free-standing blended solid polymeric thin films

Anil Arya[1] · Mohd Sadiq[1,2] · A. L. Sharma[1]

Received: 14 August 2018 / Revised: 27 November 2018 / Accepted: 1 December 2018

Abstract

Blended solid polymeric thin films based on PEO–PVP complexed with LiBOB were synthesized by solution cast technique. The effect of salt on morphology, structure and electrochemical properties was examined. The XRD and FESEM analyses reveal the enhancement of amorphous content on salt addition. The FTIR spectroscopy evidences the complex formation and presence of various microscopic interactions. The ionic conductivity for the optimized system has been estimated and found to be two orders higher than the salt-free system, i.e., $\sim 5.1 \times 10^{-6}$ S cm^{-1} (@40 °C), and remains increasing with temperature i.e. 6.5×10^{-4} S cm^{-1} (@100 °C) for O/Li = 16. The enhancement of ionic conductivity is attributed to increase in the number density of mobile ions as concluded by the Rice and Roth model. The high t_{ion} (~ 0.99) evidences the ionic nature of complexed electrolyte. DSC analysis evidences the suppression of crystallinity and shift of glass transition and melting temperature toward lower temperature implies the enhancement of the amorphous content and forms the rubbery nature of the thin films which support the faster ion conductions. Finally, an interaction scheme is proposed for a better explanation of the ion transport on the basis of experimental findings.

Keywords Blended solid polymeric thin films · Ionic conductivity · Glass transition temperature · Relaxation time

Introduction

The lithium-ion batteries (LIBs) technology is most revolutionary technology that encounters the demand of both stationary and dynamic (S&D) energy storage (like electric vehicles (EVs), portable electronics and storing of wind/solar energy) for

✉ A. L. Sharma
alsharma@cup.edu.in

[1] Department of Physical Sciences, Central University of Punjab, Bathinda, Punjab 151001, India

[2] Department of Physics, A R S D College, Delhi 11021, India

Published online: 10 December 2018

humankind all over the globe. The conventional LIBs system consists of two electrodes separated by organic salt (electrolyte) kept in an organic/inorganic separator. The electrolyte provides medium for shuttling of lithium ions between electrodes. But the liquid electrolyte is not appropriate, subject to safety problems such as poor mechanical strength, low decomposition voltage, instability, dendrite growth formation, high reactivity, flammability, leakage and bulky size. The goal is to replace the liquid section with solid polymer electrolyte which seems to be a most promising alternate option that is getting the marvelous consideration from the scientists in the field. One unique advantage of the polymer is that the cell construction in the desired shape becomes easy. Solid polymer electrolytes (SPEs) are a suitable substitute that may overcome the safety issues, suppress dendrite growth and provide acceptable features such as lightweight, flexibility, ease of fabrication, inert toward electrodes, and may prevent from battery instability [1–5]. But the designed SPE must possess desirable ionic conductivity, broad stability window and good thermal/chemical stability. In order to achieve the above-mentioned parameters, a number of host polymers have been tried and discussed in the previously published report [6]. The prerequisite property of salts such as low lattice energy, smaller cation and bulky anion needs to be taken care during the complexation. The mechanism of polymer–salt complexation has been already reported [7].

Among previously reported polymer, the polyethylene oxide (PEO) is the most popular aspirant due to broad solubility range of salts, ease of dissolution and fast migration of cation. But the poor mechanical strength, thermal stability and high crystallinity (71%) hinder its use in the energy storage devices. The crystalline phase is not suitable for ion migration, so amorphous region is desirable as it facilitates the mutual polymer chain motion which supports the cation migration [8, 9]. In view of this, various approaches have been executed such as (1) polymer blending, (2) branching, (3) grafting, (4) cross-linking. Out of aforesaid approaches, polymer blending seems more effective, efficient and easy, as it enables us to achieve the properties of an individual component of the polymer using a common solvent. One remarkable advantage is that by varying the composition of the constituents, properties can be tailored as per the requirement. The blending of two polymers improves the mechanical stability and suppresses the crystallinity and electrical conductivity. Basically, blending lowers the reorganizational tendency of the host polymer matrix that is reflected in the enhanced ion transport via coordinating sites [10–13].

Various blend polymer systems have been investigated, such as PEO–PAN, PEO–PVdF, PVA–PEO, PEO–PEG, PVA–PVP, PVC–PEMA, PEO–PVP and PVC–PEO [14–23]. The polyvinylpyrrolidone (PVP) is chosen as blend polymer due to high amorphous content associated with it. Besides this, significant ionic conductivity, high solubility in polar solvents, good thermal stability and ability to provide faster ion migration PVP is getting more attention of the researchers [24–27]. Another most promising approach to enhance the conductivity is the use of salt with a large anion as compared to the traditional salts such as $LiClO_4$, $LiPF_6$, $LiAsF_6$, $LiBF_4$ [28–32]. In the present study, salt lithium bis(oxalate) borate "LiBOB" is chosen due to advantages, low cost, high thermal stability ($T_d = 302$ °C), environment-friendliness of its decomposition and hydrolysis products (harmless B_2O_3 and CO_2, versus toxic and corrosive HF and/or POF_3 from the fluorine-containing lithium

salts) [33–35]. The unique properties of the salt and polymer provoke us to find a suitable polymer electrolyte by combining the properties of individual constituents of solid polymer electrolyte matrix. It is worth to state the adaptability of the solid polymer electrolyte for application in battery. The ionic conductivity and stability properties can be tuned by choosing the anion or cation as both contribute to ion conduction. It is worth to mention that the moving ion plays a vital role in electrolyte where the ions migrate via the coordinating sites associated with segmental motion of polymer chain. The ionic transport in polymer electrolytes is associated with the size of cation and anion. The feasibility of use of large anion is that immobilization of the anion in polymer backbone may be achieved so that only cation behaves as active species which is desirable to reduce the concentration polarization.

In the present paper, we have successfully synthesized the blended solid polymeric thin films (PEO–PVP + LiBOB) and investigated the structural and electrical properties with different LiBOB variations. The structural and morphological changes in the blend polymer electrolyte were investigated by XRD and FESEM, respectively. The presence of polymer with salt has been investigated by FTIR analysis. The optimization of ionic conductivity was performed in a broad temperature range (40–100 °C). The ion transference number and thermal transition have been obtained by the *i–t* characteristics, DSC, respectively. An ion transport mechanism has been proposed on the basis of the experimental results.

Experimental

Materials

The polymer, PEO (av. Mol. Wt.; 200,000, Sigma), PVP (av. Mol. Wt.; 40000, Sigma), LiBOB (Mol. Wt. 167.95 g/mol, Sigma) and methanol (Loba) were used as received. The chemical structure of all material is displayed in pictorial form as shown in Fig. 1.

An appropriate amount of the polymer (80:20::0.4 g:0.1 g) and salt ($O/Li^+ = 16, 18, 20, 22, 24$) was mixed methodically using the common solvent methanol by standard solution cast technique. An appropriate amount of PEO and PVP was added in methanol (20 ml) and kept for 10 min for swelling of polymer chains followed by 4-h stirring. The addition of an appropriate amount of salt (LiBOB) stoichiometric ratio has been calculated considering oxygen of PEO and is expressed as:

$$\frac{O}{Li^+} = \frac{\text{No. of monomer units in 0.4 g of PEO}}{\text{No. of LiBOB molecules in half gram of salt}} \times \frac{\text{wt. of PEO taken}}{\text{wt. of salt}}. \tag{1}$$

Then, the appropriate stoichiometric ratio of salt ($O/Li^+ = 16, 18, 20, 22, 24$) was added to the homogeneous solution and stirred for 12 h before casting in the petri dishes. The casted films in petri dishes left for drying at room temperature in a vacuum oven (for 24 h). Finally, the dried casted thin films are peeled off from petri dishes and stored in a vacuum desiccator to avoid contamination. The stored casted thin films

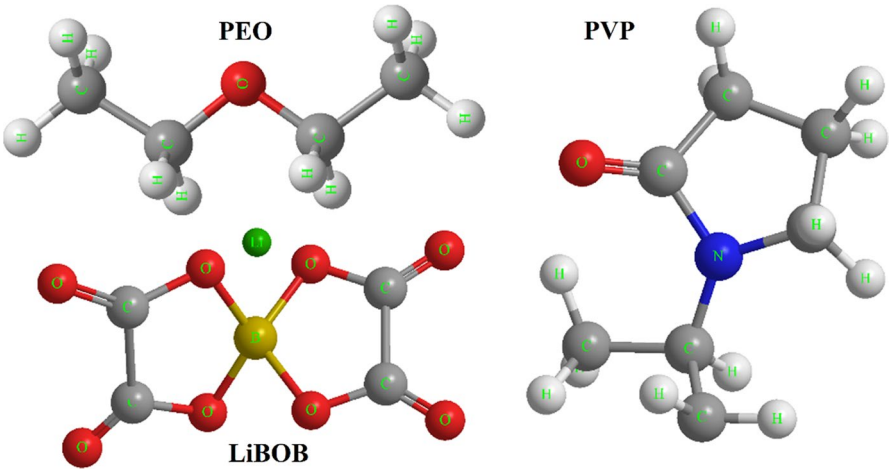

Fig. 1 Structure unit of PEO, PVP and salt LiBOB

are now put in standby for further relevant characterizations. Figure 2a, b displays the interaction mechanism of polymer–salt complex and diagram of solution cast technique by an appropriate flowchart. The polymer blending (PEO–PVP) is observed between two polymers, and the most common interactions are hydrogen bonding (shown by dotted line). Besides this, some other interactions exist, i.e., dipole–dipole interactions and ionic interactions [36].

Characterizations and basic background

X-ray diffraction

The interlayer spacing (d) and the interchain separation (R) were investigated by the (XRD) (Model: Bruker D8Advance) performed and recorded with Cu-K_α radiation ($\lambda = 1.54$ Å) in the Bragg's angle range (2θ) from 10° to 60° [37]:

$$\text{Interlayer spacing}(d) \quad 2d\sin\theta = n\lambda \tag{2}$$

and

$$\text{Interchain separation}(R) \quad R = 5\lambda/8\sin\theta. \tag{3}$$

Field emission scanning electron microscopy (FESEM) The surface morphology and the topography were investigated by the FESEM (Model: Carl Zeiss). The samples were taken in a high vacuum after sputtering with gold in order to prepare conductive surfaces.

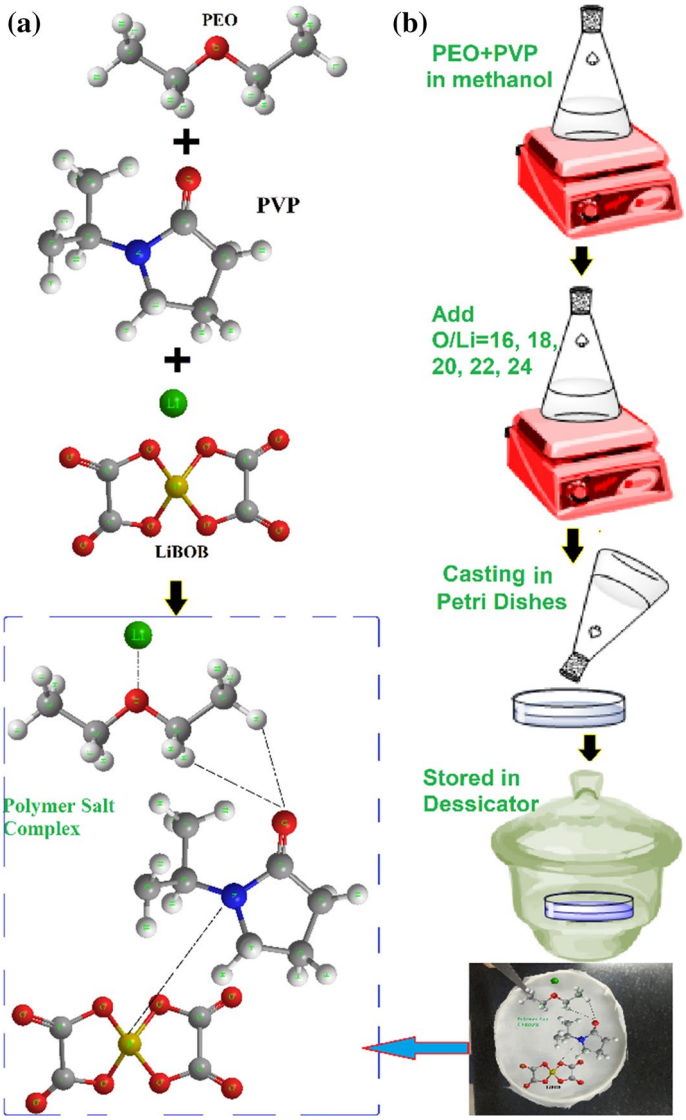

Fig. 2 **a** Representation of blend formation and cation coordination, **b** flow chart of solution cast technique

Fourier-transform infrared spectroscopy

The presence of the various interactions in the blend solid polymer electrolyte was evidenced by the FTIR (Bruker Tensor 27, Model: NEXUS–870) in absorbance mode over the wavenumber region from 600 to 3500 cm^{-1} (resolution of 4 cm^{-1}).

Impedance study

The ionic conductivity was measured by impedance spectroscopy (IS) in the frequency range of 1 Hz to 1 MHz using the CHI (Model: 760; USA) electrochemical analyzer. An AC sinusoidal signal of 20 mV was applied to the cell configuration SS|SPE|SS where solid polymer electrolytes films were sandwiched between two stainless steel electrodes. The intercept between the semi-circle at high frequency and tilted spike at low frequency was taken as the bulk resistance (R_b). The bulk conductivity (σ) value was obtained using Eq. (4):

$$\sigma_{dc} = \frac{1}{R_b}\frac{t}{A}, \tag{4}$$

where "t" is the thickness (cm) of polymer film, R_b is the bulk resistance (Ω) and A is the area (cm^2) of working electrode. The temperature-dependent conductivity was studied in the temperature range from 40 to 100 °C with a temperature difference of 10 °C (Temperature Controller; Marine India). All the samples were kept for 20 min to attain the thermal equilibrium before each measurement. The thermal activation energy for ionic transport was estimated from the slope of the linear fit of the Arrhenius plot. The linear variation in log (σ/S cm^{-1}) versus 1000/T plot suggests a thermally activated process represented by Arrhenius Equation (5):

$$\sigma = \sigma_o \exp\left(-E_a/kT\right), \tag{5}$$

where σ_o is the constant pre-exponential factor and E_a is the activation energy. The parameter T stands for the absolute temperature and k for the Boltzmann constant.

Differential scanning calorimetry study

To evaluate the glass transition temperature, melting temperature and the crystallinity, DSC (Model: DSC-Sirius 3500) was performed with a heating rate of 10 °C min^{-1} under an N_2/Ar atmosphere. Solid polymer electrolyte films with the weight of 8–10 mg were sealed in aluminum pans, and an empty sealed aluminum pan was used as a reference. The crystallinity was calculated using Eq. (6):

$$X_c = \frac{\Delta H_m}{\Delta H_m^o} \times 100, \tag{6}$$

where ΔH_m is the melting enthalpy obtained from the DSC measurement and ΔH_m^o is the melting enthalpy of pure 100% crystalline PEO (188 J/g) [8, 38].

Ion transference number study

The total ionic transference number (t_{ion}) was obtained by placing polymer electrolyte film between stainless steel (SS) blocking electrodes, and a fixed dc voltage of 10 mV was applied across the SS|SPE|SS cell (@ 40 °C). Ion transference numbers of the solid polymer electrolytes was evaluated using Eq. (7) on SS|SPE|SS cell:

$$t_{\text{ion}} = \left(\frac{I_t - I_e}{I_t}\right) \times 100. \tag{7}$$

The samples are labeled as PP, PP16, PP18, PP20, PP22 and PP24 for blend solid polymer electrolyte films with $\ddot{O}/Li^+ = 0, 16, 18, 20, 22, 24$ of LiBOB, respectively, for further investigation.

Results and discussion

X-ray diffraction (XRD)

The XRD spectra of the PEO–PVP blend polymer electrolyte with different salt contents are presented in Fig. 3. The most intense peaks located at 19.36° and 23.72° are associated with the PEO, corresponding to the plane (120) and (112), and represent the crystalline phase of the PEO due to the presence of strong hydrogen bonding. Then, a low-intensity peak at 15°, 26° and 27° of PEO are associated with the plane (013), (222) and (111), respectively [39]. The presence of a small peak in the blend polymer located at 13° is attributed to the amorphous nature of PVP. Further addition of salt leads to the disappearance of peak, and it confirms the multiphase (both crystalline and amorphous phases). The salt addition in the blend polymer

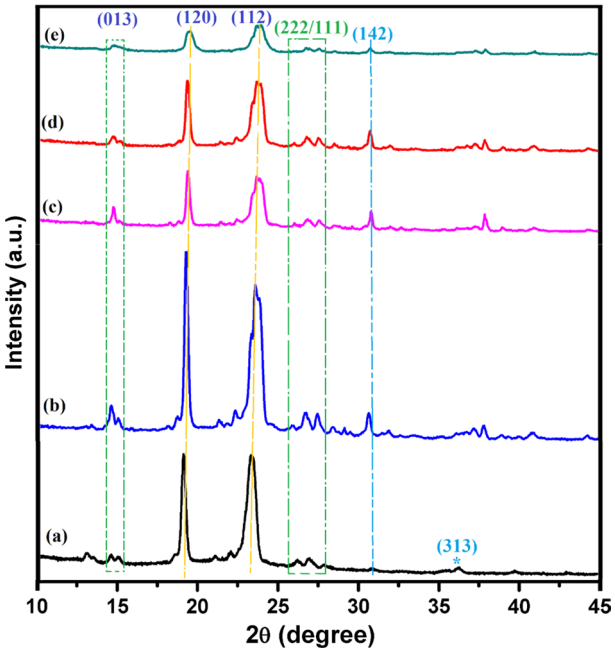

Fig. 3 XRD patterns of blend polymer electrolyte films with LiBOB (O/Li) = (a) 0, (b) 24, (c) 22, (d) 20, (e) 16

electrolyte alters the peak intensity and position that confirms the formation of polymer–salt complex due to polymer–salt interaction. The decrease in intensity associated with the most intense peak of PEO suggests the decrease in the crystallinity. It may be due to the interaction of the cation with the polymer chain that disrupts the ordered arrangement of the polymer chain and strengthens the amorphous content. Further, the disappearance of the salt peak confirms the complete dissolution of the salt in the polymer matrix and good miscibility [40]. The *d*-spacing between the diffraction planes was obtained using Eq. (2) and interchain separation (*R*) using Eq. (3), and the determined values are given in Table 1.

It may be observed from Table 1 that the *d*-spacing and the interchain separation are varying slightly on the addition of the salt that indicates that the covalent bonding between the polymer chain is disrupted that results in the lowering of the polymer chain viscosity and hence the faster ion migration is achieved [7]. It suggests that the polymer–salt complexation occurs and salt effectively modifies the polymer chain arrangement that confirms the enhancement of the amorphous content which is desirable for faster on migration that will be reflected in the impedance spectroscopy section.

Field emission scanning electron microscopy (FESEM)

The field emission scanning electron microscopy (FESEM) technique is performed to investigate the morphology and the elemental composition by the energy-dispersive X-ray spectroscopy (EDS). Figure 4 displays the FESEM micrographs of the blend polymer electrolyte films. Figure 4a shows the micrograph of the pure PEO, and rough/rigid structure indicates the crystalline nature of the PEO. When PVP is added to the PEO, the surface roughness is disrupted and the modified surface is observed that indicates the blend formation. The blend formation is associated with the presence of hydrogen interaction and ionic interactions (Fig. 4b). The absence of the cracks and formation of the smooth surface indicate the polymer miscibility due to hydrogen bonding between the polymers. Further addition of the salt modifies the surface morphology and indicates the formation of the polymer–salt complex via the coordinating interaction of the lithium ion with ether group of PEO [41]. The uniform distribution of the salt in the polymer matrix enhances the amorphous phase

Table 1 Values of Bragg's angle 2θ, Basal spacing (d) and interchain separation (R) corresponding to 120 and 112 reflection planes of PEO in blend solid polymer electrolyte films

Sample code	PEO 120 reflection plane parameters			PEO 112 reflection plane parameters		
	2θ (°)	d (Å)	R (Å)	2θ (°)	d (Å)	R (Å)
PP	19.1	4.65	5.81	23.1	3.85	4.81
PP24	18.9	4.67	5.84	23.1	3.84	4.80
PP22	18.9	4.67	5.84	23.1	3.83	4.79
PP20	18.9	4.68	5.85	23.1	3.83	4.79
PP16	18.9	4.67	5.83	23.1	3.83	4.78

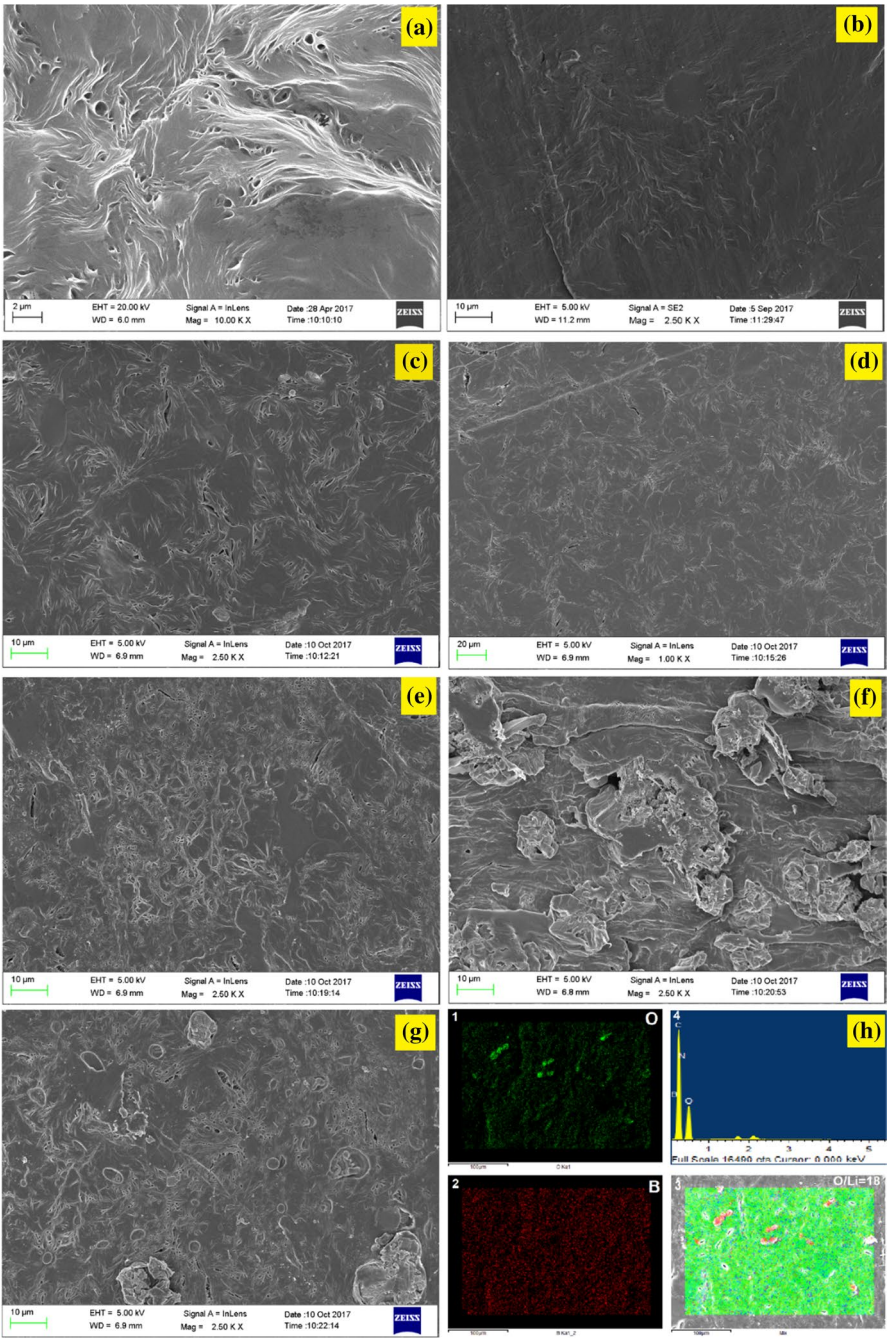

Fig. 4 FESEM micrographs of the **a** PEO, **b** blend polymer electrolyte (PEO–PVP), **c**–**g** blend PEO–PVP with O/Li = 0, 16, 18, 20, 22, 24 of LiBOB and **h** elemental mapping and EDX spectra of the O/Li = 16

and is evidenced by the XRD analysis. For better visibility of the salt dissociation, EDS has been performed and it confirms the uniform presence of the salt in the polymer matrix. Further, the elemental composition of the O and B of the salt suggests complete dissolution of the salt (Fig. 4h). It might be concluded that the addition of the salt alters the ordered arrangement of the polymer chains and smoother surface facilitates the faster ion migration.

Fourier-transform infrared spectroscopy (FTIR)

The presence of various functional groups in the polymer–salt complex comprising PEO–PVP + LiBOB is observed by the FTIR spectra. Figure 5 displays the FTIR spectra of the blend polymer (a) and complexed with different salt contents (b–f). The spectral region in the wavenumber range 600–1600 cm^{-1} consists of the CH_2

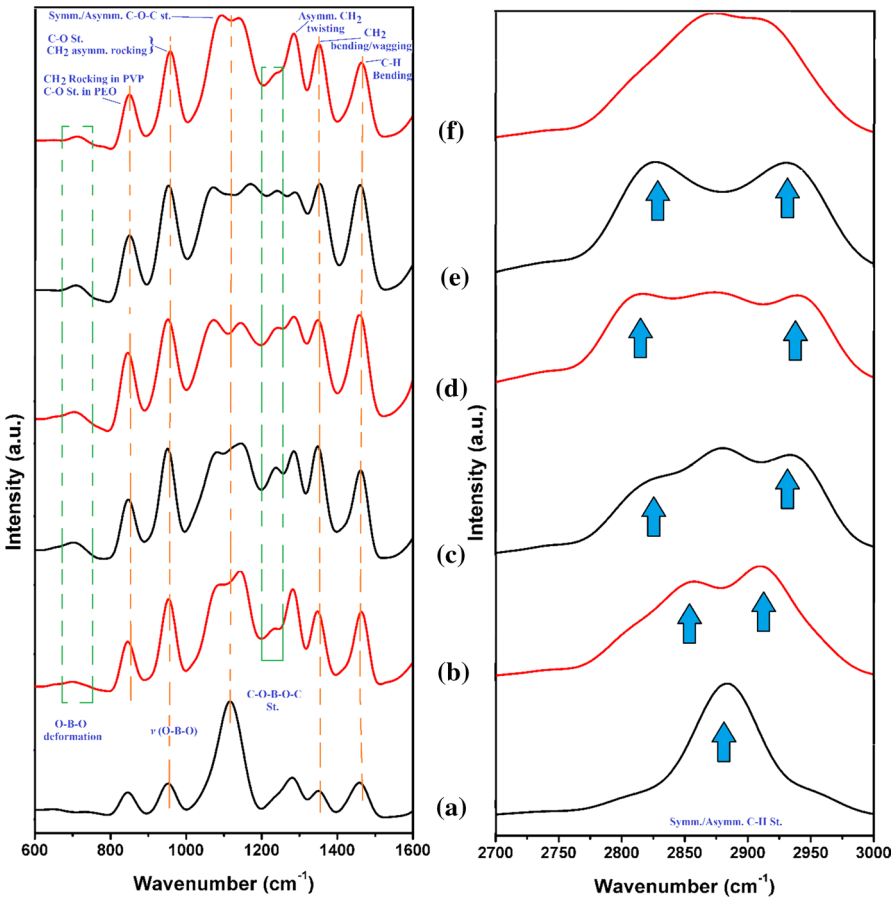

Fig. 5 FTIR spectra of blend polymer electrolyte films with O/Li ratio (a) 0, (b) 16, (c) 18, (d) 20, (e) 22, (f) 24

rocking, C–O st., CH_2 asymm. rocking, C–O–C st. symm/asymm., CH_2 twisting and wagging mode. The band observed at the 846 cm^{-1} is associated with the CH_2 rocking mode and some contributions from the C–O stretching mode. The band located at the 958 cm^{-1} is attributed to the symm./asymm. stretching mode of C–O–C band. The band observed at the 1280 cm^{-1}, 1340 cm^{-1} and 1480 cm^{-1} corresponds to the CH_2 (asymm. twisting), CH_2 bending/wagging and C–H bending, respectively. Addition of the low salt to the blend polymer electrolytes alters the peak position and intensity that indicates that the salt plays an effective role in altering the polymer arrangement. The change in the characteristics peak of polymer implies the disruption of polymer chain conformation which infers the polymer–salt complex formation [41, 42].

The C–O–C st. observed at 1100 cm^{-1} indicates the amorphous nature, and after the addition of salt the peak gets broadened and is asymmetric that strongly evidences that the cation is going to coordinate with the ether group of PEO than the PVP. This also confirms that the PEO has a high probability of attracting the cation and ether group acts as a strong electron donor. The overall effect is the disruption of the ordered arrangement of the polymer chains, and amorphous content is increased and is in agreement with the XRD results which show a reduction in the peak intensity and hence the crystallinity. It suggests that the addition of the salt modifies the polymer chain arrangement via the coordinating interaction between the cation and the electron-rich group of the PEO. The ether group promotes the salt dissociation in the blend polymer matrix. This interaction alters the peak position and intensity which indicates that the polymer crystallinity is disrupted. Now, the presence of BOB^- group in LiBOB has led to the 10 Raman and 7 IR active vibrational modes. The main band is observed (Fig. 5) at 775, 985, 1089 and 1400 cm^{-1} attributed to the O–B–O deformation, ν(O–B–O) + δ(O–C–O), O–B–O symmetric stretch and B–O extra-ring stretch, respectively [43–45]. The change in the anion peak with an increase in salt content is observed in terms of the change in the peak shape and the negligible change in position in the blend polymer electrolyte. Figure 6 depicts the deconvolution spectra of the anion peak in the wavenumber region of 1700–1850 cm^{-1}, and peaks are associated with the C=O stretch of the LiBOB. Another important region is the 2800–2900 cm^{-1} and is associated with the symm/asymm. C–H stretching of the PEO. For the blend polymer, a symmetrical peak is observed and the addition of salt disrupts the symmetry of the peak and two peaks can be observed that suggests that the salt plays an effective role in altering the blend polymer electrolyte (Fig. 6b–f). In totality, it may be summarized that the incorporation of the salt in the blend polymer electrolyte alters the structure of polymer matrix and interaction between the polymer and salt is modified. It may also be concluded that the polymer–salt complexation occurs which is evidenced by the XRD and FESEM analysis too. Further investigation regarding the modification of the structure is analyzed by evaluating the glass transition temperature, melting temperature and crystallinity in "Differential Scanning Calorimetry (DSC)" section.

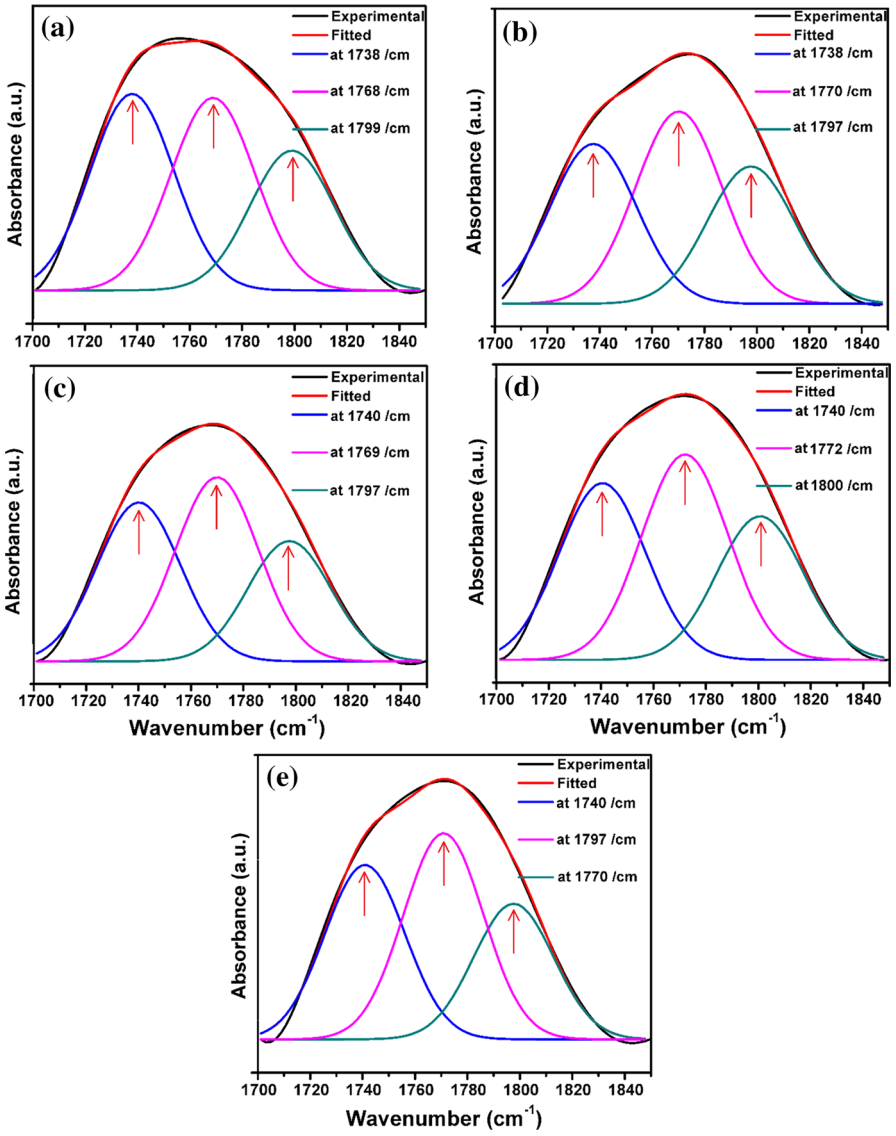

Fig. 6 FTIR deconvolution of the C=O peak of salt for O/Li ratio **a** 16, **b** 18, **c** 20, **d** 22, **e** 24

Impedance spectroscopy (IS)

The electrical conductivity of the prepared solid polymer electrolyte (PEO–PVP) with different salt contents (LiBOB) has been measured via impedance spectroscopy in a broad temperature range (40–100 °C @ 10 °C). The impedance spectroscopy has been performed by sandwiching the thin films between two stainless steel blocking electrodes (inset of Fig. 7a). A small ac signal (~ 20 mV) is applied

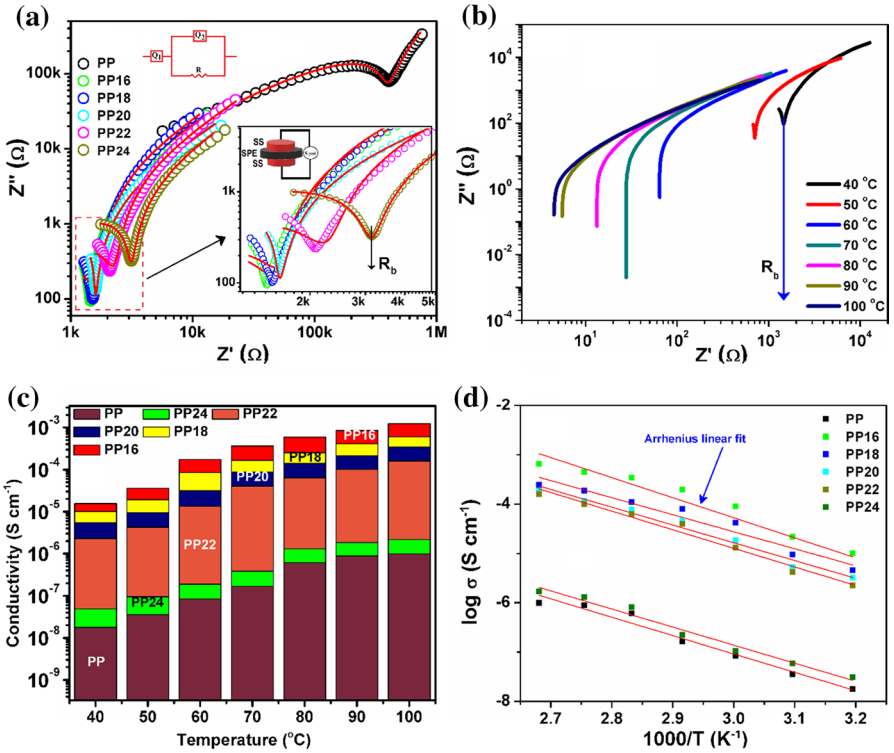

Fig. 7 **a** Impedance plot of blend polymer electrolyte with different salt content, **b** temperature variation of PP16 blend polymer electrolyte, **c** variation of conductivity against temperature for different salt content, **d** reciprocal temperature dependence of the conductivity for blend polymer electrolyte

across the SS electrodes, and the plot of the imaginary part versus the real part of impedance is observed in the frequency range 1 Hz to 1 MHz. Figure 7a summarizes the impedance plot which comprises the two regions depending on frequency, one high-frequency arc associated with the bulk property of electrolyte (associated with ion migration) followed by the tilted spike of the low frequency that is associated with the electrode double-layer capacitance of the electrodes or interfacial phenomena [41, 46–48]. A reduction in the high-frequency arc and an increase in the low-frequency arc with salt addition indicate the decrease in resistivity. The minima in the imaginary part of the impedance (Z'') correspond to the bulk resistance (R_b).

The impedance plot of the prepared solid polymer electrolyte is fitted (solid red line) with equivalent circuit element (shown in inset) and is in absolute agreement with the experimental data (data points). The equivalent circuit element comprises constant phase element (Q_1) in series with the parallel combination of constant phase element (Q_2) and resistance (R_b). The magnitude of the fitted parameters is summarized in Table 2. It may be noted that the bulk resistance is minimum for the solid polymer electrolyte with O/Li = 16 salt concentration and

Table 2 Fitted parameters, different contributions of electrical conductivity (ionic and electronic) and transference number for blend solid polymer electrolyte

Sample code	Fitted parameters of equivalent circuit element					t_{ion} @ 40 °C	Electrical conductivity (S cm^{-1})		$\sigma_{electronic}$ (S cm^{-1})	σ_{ionic} (S cm^{-1})
	R_b (kΩ)	Q_1	n_1	Q_2	n_2		@ 40 °C	@ 100 °C		
PP	398.1	4.0×10^{-7}	0.58	1.3×10^{-10}	0.82	–	1.7×10^{-8}	9.8×10^{-7}	–	–
PP24	3.079	1.6×10^{-4}	0.59	1.6×10^{-8}	0.80	0.95	3.1×10^{-7}	1.1×10^{-6}	1.1×10^{-9}	2.9×10^{-8}
PP22	2.410	5.6×10^{-6}	0.71	6.2×10^{-9}	0.44	0.95	2.2×10^{-6}	1.5×10^{-4}	1.2×10^{-9}	2.1×10^{-6}
PP20	1.794	1.2×10^{-6}	0.63	8.3×10^{-10}	0.80	0.98	3.5×10^{-6}	1.8×10^{-4}	7.1×10^{-8}	3.4×10^{-6}
PP18	1.661	7.7×10^{-6}	0.79	3.1×10^{-4}	0.32	0.99	4.5×10^{-6}	2.4×10^{-4}	4.5×10^{-8}	4.5×10^{-6}
PP16	1.594	8.5×10^{-6}	0.80	2.2×10^{-5}	0.33	0.99	5.1×10^{-6}	6.5×10^{-4}	4.8×10^{-8}	4.8×10^{-6}

is optimum concentration. The temperature variation of the optimized system is shown in Fig. 7b. It may be noted that with an increase in the temperature low-frequency arc dominates, while the high-frequency arc is masked. The former one suggests that the charge carriers in the polymer matrix are ions and predominantly contributed to total conductivity. It confirms the dominance of diffusion process over capacitive nature [49]. The decrease in bulk resistance is observed and is attributed to the increased polymer flexibility which promotes faster ion migration due to thermal activation of charge carriers [50]. In addition, it is also seen from the plot that bulk resistance decreases with the addition of the salt to the polymer matrix. The lowest value was recorded for the PP16. The addition of salt provides more free charge carriers in the polymer matrix, and available charge carriers participate in the conduction process; hence, an increase in the conductivity is observed (Fig. 7a).

Therefore, in comparison with the blended polymer electrolyte without salt, blended polymer electrolyte with salt displays increased conductivity which is possible only when the polymer matrix has amorphous content, faster ion mobility and enhanced polymer flexibility. The conductivity is calculated using Eq. (4) and summarized in Table 2. The highest ionic conductivity of 5.10×10^{-6} S cm^{-1} at 40 °C is observed for PP16. The ionic conductivity value was higher than the PEO–PVP + LiClO4-based system which displays a conductivity of 3.7×10^{-6} S cm^{-1} at 40 °C [51]. It may be concluded that the conductivity increases with the addition of salt and is maximum for the O/Li = 16-based electrolyte. The increase in conductivity with salt addition is also in agreement with the relation: $\sigma = ne\mu$, where n is the number of charge carriers, e is the charge and μ is the ion mobility. Due to polymer–salt interaction, salt gets separated into cation and anion. The cation due to a smaller size is only active species, and anion having large size is immobilized with the polymer backbone owing to the higher Coulombic potential and low segmental self-mobility [52]. It infers the enhancement of ionic conductivity and is also in good agreement with the DSC analysis.

Table 3 Comparison of the ionic conductivity of various sodium and lithium salts

Polymers	Salt	Ionic conductivity (S cm^{-1})	Temperature	References
PEO–PMMA	$LiBF_4$	10^{-6}	27 °C	[53]
PEO–PVP	$NaIO_4$	1.56×10^{-7}	RT	[54]
PEO–PVP	NaF	1.19×10^{-7}	RT	[55]
PEO–PEMA	$NaClO_4$	6.77×10^{-7}	30 °C	[56]
PVC–PEMA	$NaIO_4$	10^{-8}	RT	[57]
PEO–PVP	NaBr	1.90×10^{-6}	RT	[39]
PEO–PVP	$LiClO_4$	3.77×10^{-6}	40 °C	[58]
Chitosan–methylcellulose blend	$LiBF_4$	3.74×10^{-6}	–	[59]
PEO–PVP	LiBOB	5.1×10^{-6}	40 °C	Our work
PEO–PVP	LiBOB	6.5×10^{-4}	100 °C	Our work

Solid polymer electrolyte with high salt concentration (i.e., O/Li > 14 or 12) is unable to form a film. It may be concluded that the O/Li = 16-based solid polymer electrolyte is the optimized system. A comparison of ionic conductivity for various blend polymer matrixes and different salts is summarized in Table 3. It may be noted that the present system possesses comparatively higher ionic conductivity and may be used for the practical application.

Figure 7c depicts the temperature variation (40–100 °C) of bulk (DC) conductivity for blend polymer electrolyte with different salt concentrations and is two orders higher at 100 °C (6.5×10^{-4} S cm^{-1}) as compared to 40 °C (5.1×10^{-6} S cm^{-1}). It may be noted that conductivity increases with the increase in temperature and is ascribed to the following reasons: (1) increased polymer flexibility, (2) higher free volume, (3) enhanced segmental motion of polymer chain ascribed to the bond rotation and (4) improved salt dissociation. This enhancement of the conductivity is in absolute agreement with the Rice and Roth model [60, 61]. It expresses the ionic conductivity via Eq. (8)

$$\sigma = \frac{2}{3}\left[\frac{(Ze)^2}{k_B T m}\right]\eta E_a \tau \exp\left(-\frac{E_a}{k_B T}\right), \tag{8}$$

where σ, η, Z, e, E_a, m, T, k_B, e and τ represent the conductivity, density, charge carrier, elementary charge, activation energy, the mass of the conducting ions, absolute temperature, Boltzmann constant, electronic charge and time travel of ions between sites, respectively. It suggests that ionic conductivity is in direct relation to the number of free ions.

Figure 7d depicts the temperature dependence of the ionic conductivity and follows the Arrhenius behavior (Eq. 5). As the temperature increased, the ion migration from one coordination site to another occurs fast due to thermal activation and is associated with the lowering of the activation energy. The solid line in the plot shows the Arrhenius fit. The lowering of the activation energy evidences the significant increase in the ionic conductivity as compared to the blend polymer electrolyte without salt [41]. Lowering in the activation energy suggests the availability of a favorable path for cation migration, and conductivity reaches ~6.5×10^{-4} S cm^{-1} at 100 °C (for PP16) which lies within the functioning range of the solid-state battery. So, it may be suggested that both salt concentration and temperature are the key players that control the ion transport in the blend polymer matrix.

The double-layer capacitance was obtained from the minima in the imaginary part of the impedance ($C_{dl} = -1/\omega Z''$), and relaxation time ($\tau = 1/\omega$) was obtained using the frequency corresponding to minima in the imaginary part of the impedance. Figure 8 shows the plot of double-layer capacitance and relaxation time for different salt contents. It is observed that the solid polymer electrolyte with salt addition displays the highest double-layer capacitance and lowest relaxation time [62, 63]. The former suggests the effective salt dissociation in the cation/anions due to polymer–salt interaction, while the latter indicates the fast ion dynamics due to the fast segmental motion of the polymer chain. The reduction in relaxation

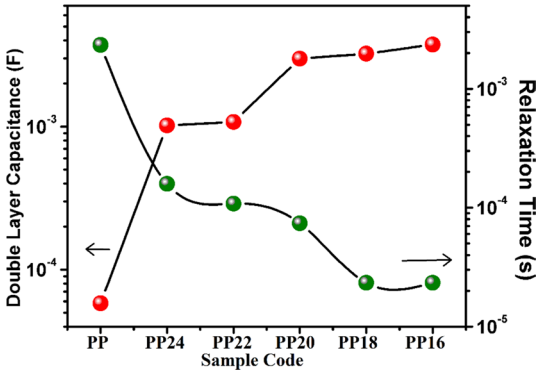

Fig. 8 Plot of double-layer capacitance and relaxation time for the solid polymer electrolyte with different salt concentration

time directly indicates the increased rate of ion hopping which agrees well with the conductivity study.

Above investigations support the FTIR results which evidence the lowering of the interaction between cation and anion and salt dissociation increases. This separates the cation and anion. Therefore, the amorphous phase in the blend polymer matrix allows the cation migration supported by the segmental motion of polymer chains, while the anion is attached to the polymer backbone. This leads to an increase in the conductivity and polymer flexibility, while displays a reduction in crystallinity as evaluated from XRD. The large anion of the LiBOB facilitates the improved electrical properties as expected. To further support the ionic conductivity, DSC was perfomed as discussed in the forthcoming section.

Differential scanning calorimetry (DSC)

Figure 9 illustrates the DSC thermograms of the blend polymer electrolyte films with different salt contents. DSC is used to calculate the glass transition temperature (T_g), crystallinity (X_c) and the melting temperature (T_m). From Fig. 9, the onset T_g was observed in the range of 45–60 °C. As it is well known that the T_g of the PEO is −57.6 °C and of PVP is 69 °C, the present system displayed only a single T_g between the individual polymers that confirms the miscibility of the polymer. The motion of polymer chains is the key player that facilitates the cation migration and is evidenced by the glass transition temperature value. Addition of salt lowers the T_g, and it indicates that the polymer flexibility increases due to the interpenetration of the anion between the polymer chains (Table 4). The increased flexibility is an indication of the amorphous phase that is desirable for the fast solid-state ionic conductor [46, 64]. The relative crystallinity was calculated from the DSC thermogram using Eq. (6). It is observed that the addition of salt lowers the crystallinity. The lowering of the crystallinity is attributed to the coordination interaction between the polymer chain and the cation (Li^+). As FTIR also evidenced the cation coordination with the electron-rich group of the polymer chain and anion with polymer backbone, both cation and anion together alter the polymer chain arrangement and more free

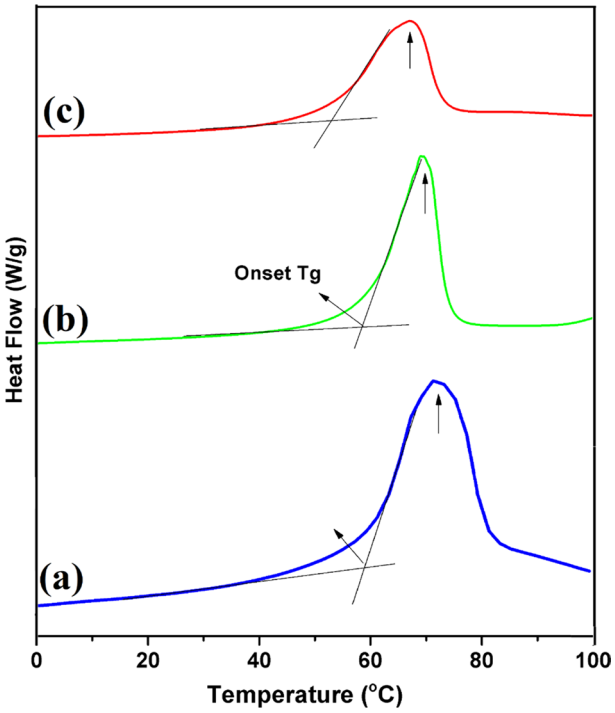

Fig. 9 DSC thermograms of (a) PEO–PVP, (b) O/Li = 20 and (c) O/Li = 16

Table 4 Glass transition temperature, crystallinity and the melting temperature of the blend polymer electrolyte and blend polymer electrolyte with salt content

Sample code	T_g (onset, °C)	T_m (°C)	X_c (%)
PP	59.78	71.7	66.75
PP20	57.89	69.2	53.29
PP16	53.17	67.1	49.09

volume is available for the cation migration [41, 64]. Above results are also confirmed by the XRD analysis as shown in Fig. 3.

The decrease in crystallinity is linked directly to the polymer flexibility and the segmental motion of the polymer chains. The reduction in crystallinity is also observed in the XRD analysis. The melting temperature peak also shows shifts toward the lower temperature on the addition of the salt. It may be attributed to the lowering of the crystallinity and chain stiffness. The blend polymer electrolyte (BPE) complexed with salt displays the lowering of glass transition temperature, melting temperature and crystallinity. This decrease is attributed to the cation interaction with the ether group of PEO which disrupts the ordered arrangement of the polymer chains. The observed decrease in all three parameters suggests that the investigated system has faster ion migration rate which is seen in terms of the increase in conductivity and transference number.

Transference number

As a polymer electrolyte system, both ions and electrons contribute to the total conductivity. So, to separate out the ionic and electronic contribution, a well-established DC polarization method has been performed by placing the solid polymer electrolyte in between the stainless steel (SS) electrodes and a signal of 20 mV is used to be applied.

Figure 10 displays the plot of the polarization current versus time for all systems. All the plots depict the same trend of decrease in the current with time followed by a steady state for a long time. Actually, on the application of the field along with the cell configuration, all ions are accumulated on the interface due to polarization and further ion migration is blocked [65–67]. So, only active species now left is with electrons only. All the systems show a high value of ion transference number (~99%) obtained by Eq. (7) in Table 2. This implies that the total conductivity in the present system is mainly due to the flow of ions with negligible electron contribution.

Self-proposed mechanism for ion transport

Figure 11 displays the ion transport mechanism of the investigated system. Figure 11a depicts the PEO chain and the PVP chain. The blend formation is depicted in Fig. 11a, where the oxygen of the PVP chain interacts with the methyl group of the PEO chain via hydrogen bonding and ionic interactions. The blend formation

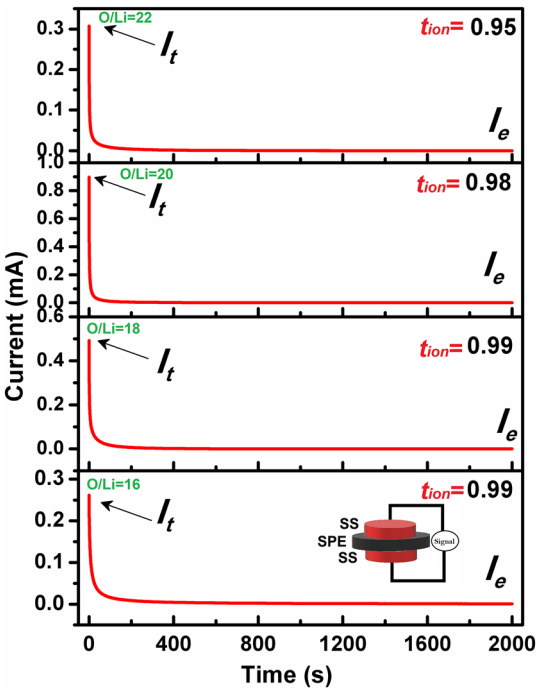

Fig. 10 Ion transference number of blend polymer electrolyte films

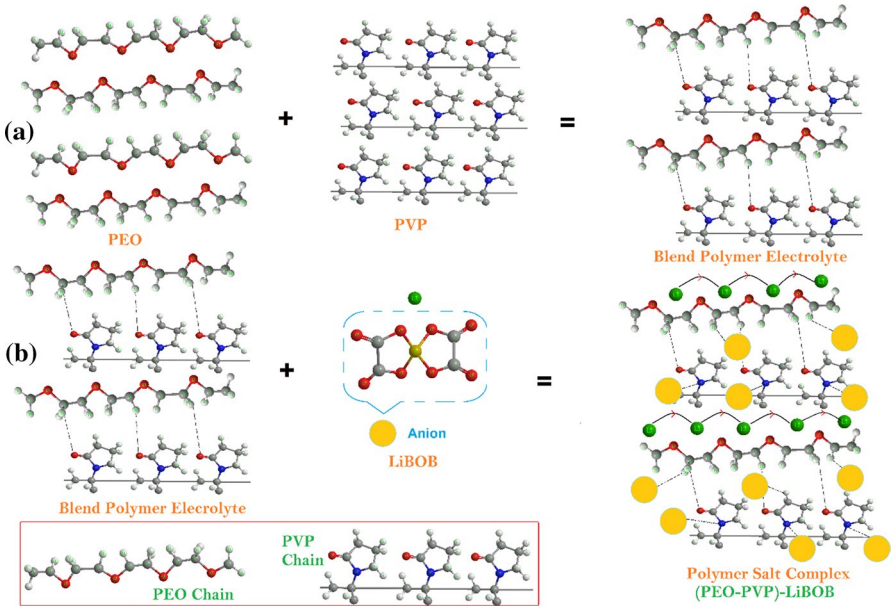

Fig. 11 Model for the lithium (Li^+) migration, **a** blend formation interaction mechanism and **b** polymer–salt complex formation

at some level alters the polymer chain arrangement which facilitates the more free space for ion migration. The blend formation is also confirmed in the XRD and FESEM results. Now, when salt is added to the blend polymer matrix, the salt gets separated into cation and anion. From here, two possibilities arise for the interaction of cation: (1) interaction with ether group of PEO and (2) with the oxygen PVP. But, from the FTIR spectra, it was evidenced that the cation coordination seems to be with the ether group of the PEO.

As it is evidenced by FTIR results, the principal peak of the PEO at 1100 cm^{-1} shows asymmetry on the addition of salt which is a clear indication that the ether group of PEO is the preferable site of coordination. Now, another species that remains is an anion. As anion is of large size, it gets attached to the polymer backbone and remains in the immobilized state (Fig. 11b). The overall effect of the salt addition is disruption of the polymer chain arrangement that indicates the enhancement of the amorphous content as evidenced by the XRD and DSC results. It can be summarized that the cation migration occurs via the coordinating sites provided by PEO, while PVP supports the backbone of the PEO. Now, when the salt content is varied, a number of charge carriers participate in conduction that results in improvement in electrical conductivity. Further, the decrease in glass transition temperature and crystallinity with the addition of salt suggests the increase in polymer flexibility/faster segmental motion of polymer chain which leads to faster ion migration.

Conclusions

In summary, solid blend polymer electrolyte based on PEO–PVP and LiBOB was synthesized by the standard solution cast technique. The X-ray diffractions analysis confirmed the reduction in the crystallinity and increase in the interchain separation that is associated with the enhanced amorphous content. The FESEM analysis confirmed the blend formation as evidenced by the alteration in morphology. The XRD and FESEM analyses confirmed the complex formation. The FTIR spectra depict the presence of the polymer-ion interactions in between the polymer and salt. The impedance study shows enhancement of the ionic conductivity, and the highest is exhibited by the blend polymer with O/Li = 16 salt content in the order of 10^{-5} S cm^{-1}. The enhancement of the ionic conductivity is attributed to the increase in a number of ion charge carriers and ion mobility. The temperature dependence of the ionic conductivity follows Arrhenius behavior, and activation energy decreases with the addition of the salt which implies the faster ion migration from one coordinating site to another. The blend polymer system with the highest ionic conductivity shows lowest relaxation time which indicates the faster ion dynamics. The high value of the ion transference number confirms the ionic nature of the prepared polymer electrolyte system. The lowering of the glass transition temperature and melting temperature indicates the enhancement of the amorphous content and is in absolute agreement ionic conductivity value. The ion transport mechanism based on the experimental results evidences the effective role played by salt in promoting ion dynamics. All the above-stated properties make the present polymer electrolyte a potential candidate as an electrolyte-cum-separator of lithium-ion battery.

Acknowledgements One of the authors, AA, is thankful to the Central University of Punjab for providing fellowship and partial funding from the UGC Startup Grant (GP-41).

References

1. Goodenough JB, Singh P (2015) Review—solid electrolytes in rechargeable electrochemical cells. J Electrochem Soc 162:A2387–A2392
2. Lin X, Salari M, Arava LMR et al (2016) High temperature electrical energy storage: advances, challenges, and frontiers. Chem Soc Rev 45:5848–5887
3. Aldalur I, Zhang H, Piszcz M et al (2017) Jeffamine®based polymers as highly conductive polymer electrolytes and cathode binder materials for battery application. J Power Sources 347:37–46
4. Gittleson FS, El Gabaly F (2017) Non-faradaic Li^+ migration and chemical coordination across solid-state battery interfaces. Nano Lett 17:6974–6982
5. Liu W, Lin D, Sun J et al (2016) Improved lithium ionic conductivity in composite polymer electrolytes with oxide-ion conducting nanowires. ACS Nano 10:11407–11413
6. Arya A, Sharma AL (2017) Polymer electrolytes for lithium ion batteries: a critical study. Ionics 23:497–540
7. Arya A, Sharma AL (2018) Structural, microstructural and electrochemical properties of dispersed-type polymer nanocomposite films. J Phys D Appl Phys 51:045504
8. Arya A, Sharma AL (2017) Insights into the use of polyethylene oxide in energy storage/conversion devices: a critical review. J Phys D Appl Phys 50:443002
9. Arya A, Sharma AL (2018) Structural, electrical properties and dielectric relaxations in Na^+-ion-conducting solid polymer electrolyte. J Phys Condens Matter 30:165402

10. Manthiram A, Yu X, Wang S (2017) Lithium battery chemistries enabled by solid-state electrolytes. Nat Rev Mater 2:16103
11. Paranjape N, Mandadapu PC, Wu G, Lin H (2017) Highly-branched cross-linked poly(ethylene oxide) with enhanced ionic conductivity. Polymer 111:1–8
12. Tao C, Gao MH, Yin BH, Li B, Huang YP, Xu G, Bao JJ (2017) A promising TPU/PEO blend polymer electrolyte for all-solid-state lithium ion batteries. Electrochim Acta 257:31–39
13. Kesavan K, Mathew CM, Rajendran S (2014) Lithium ion conduction and ion-polymer interaction in poly (vinyl pyrrolidone) based electrolytes blended with different plasticizers. Chin Chem Lett 25:1428–1434
14. Choi BK, Kim YW, Shin HK (2000) Ionic conduction in PEO–PAN blend polymer electrolytes. Electrochim Acta 45:1371–1374
15. Bhatt C, Swaroop R, Arya A, Sharma AL (2015) Effect of nano-filler on the properties of polymer nanocomposite films of PEO/PAN complexed with NaPF6. J Mater Sci Eng B 5(11–12):418–434
16. Joge P, Kanchan DK, Sharma P, Gondaliya N (2013) Effect of nano-filler on electrical properties of PVA–PEO blend polymer electrolyte. Indian J Pure Appl Phys 51:350–353
17. Arya A, Sharma S, Sharma AL, Kumar D, Sadiq M (2016) Structural and dielectric behavior of blend polymer electrolyte based on PEO–PAN + LiPF6. Asian J Eng Appl Technol 5(1):4–7
18. Premalatha M, Vijaya N, Selvasekarapandian S, Selvalakshmi S (2016) Characterization of blend polymer PVA–PVP complexed with ammonium thiocyanate. Ionics 22(8):1299–1310
19. Prasanna CS, Suthanthiraraj SA (2016) Electrical, structural, and morphological studies of honeycomb-like microporous zinc-ion conducting poly (vinyl chloride)/poly (ethyl methacrylate) blend-based polymer electrolytes. Ionics 22(3):389–404
20. Kumar KN, Kang M, Sivaiah K, Ravi M, Ratnakaram YC (2016) Enhanced electrical properties of polyethylene oxide (PEO) + polyvinylpyrrolidone (PVP): Li^+ blended polymer electrolyte films with addition of Ag nanofiller. Ionics 22(6):815–825
21. Ramesh S, Ramesh K, Arof AK (2013) Fumed silica-doped poly (vinyl chloride)-poly (ethylene oxide)(PVC/PEO)-based polymer electrolyte for lithium ion battery. Int J Electrochem Sci 8:8348–8355
22. Arya A, Sadiq M, Sharma AL (2017) Effect of variation of different nanofillers on structural, electrical, dielectric, and transport properties of blend polymer nanocomposites. Ionics 24:2295–2319
23. Arya A, Sharma AL (2018) Optimization of salt concentration and explanation of two peak percolation in blend solid polymer nanocomposite films. J Solid State Electrochem 22:2725–2745
24. Vijaya N, Selvasekarapandian S, Karthikeyan S, Prabu M, Rajeswari N, Sanjeeviraja C (2013) Synthesis and characterization of proton conducting polymer electrolyte based on poly (N-vinyl pyrrolidone). J Appl Polym Sci 127(3):1538–1543
25. Joseph A, Xavier MM, Żyła G, Nair PR, Padmanabhan AS, Mathew S (2017) Synthesis, characterization and theoretical studies on novel organic–inorganic hybrid ion–gel polymer thin films from a γ-Fe_2O_3 doped polyvinylpyrrolidone–*N*-butylpyridinium tetrafluoroborate composite via intramolecular thermal polymerization. RSC Adv 7(27):16623–16636
26. Reddy CV, Han X, Zhu QY, Mai LQ, Chen W (2006) Dielectric spectroscopy studies on (PVP + PVA) polyblend film. Microelectron Eng 83(2):281–285
27. Kesavan K, Mathew CM, Rajendran S (2014) Lithium ion conduction and ion-polymer interaction in poly (vinyl pyrrolidone) based electrolytes blended with different plasticizers. Chin Chem Lett 25(11):1428–1434
28. Arya A, Sharma AL (2016) Conductivity and stability properties of solid polymer electrolyte based on PEO–PAN + LiPF6 for energy storage. Appl Sci Lett 2(2):72–75
29. Xu W, Angell CA (2001) Weakly coordinating anions, and the exceptional conductivity of their nonaqueous solutions. Electrochem Solid-State Lett 4(1):E1–E4
30. Appetecchi GB, Zane D, Scrosati B (2004) PEO-based electrolyte membranes based on $LiBC_4O_8$ salt. J Electrochem Soc 151(9):A1369–A1374
31. Abouimrane A, Davidson IJ (2007) Solid electrolyte based on succinonitrile and LiBOB interface stability and application in lithium batteries. J Electrochem Soc 154:A1031–A1034
32. Sharma AL, Thakur AK (2013) Plastic separators with improved properties for portable power device applications. Ionics 19:795–809
33. Xu K, Zhang S, Jow TR, Xu W, Angell CA (2002) LiBOB as salt for lithium-ion batteries: a possible solution for high temperature operation. Electrochem Solid-State Lett 5:A26–A29

34. Li LF, Xie B, Lee HS, Li H, Yang XQ, McBreen J, Huang XJ (2009) Studies on the enhancement of solid electrolyte interphase formation on graphitized anodes in LiX-carbonate based electrolytes using Lewis acid additives for lithium-ion batteries. J Power Sources 189:539–542
35. Wu XL, Xin S, Seo HH, Kim J, Guo YG, Lee JS (2011) Enhanced Li^+ conductivity in PEO–LiBOB polymer electrolytes by using succinonitrile as a plasticizer. Solid State Ionics 186:1–6
36. Parameswaranpillai J, Thomas S, Grohens Y (2014) Polymer blends: state of the art, new challenges, and opportunities. Characterization of Polymer Blends Wiley, New York, pp 1–6
37. Das A, Thakur AK, Kumar K (2013) Exploring low temperature Li^+ ion conducting plastic battery electrolyte. Ionics 19:1811–1823
38. Cimmino S, Di Pace E, Martuscelli E, Silvestre C (1990) Evaluation of the equilibrium melting temperature and structure analysis of poly (ethylene oxide)/poly (methyl methacrylate) blends. Die Makromolekulare Chemie: Macromol Chem Phys 191:2447–2454
39. Kumar KK, Ravi M, Pavani Y, Bhavani S, Sharma AK, Rao VN (2014) Investigations on PEO/PVP/NaBr complexed polymer blend electrolytes for electrochemical cell applications. J Membr Sci 454:200–211
40. Sharma AL, Shukla N, Thakur AK (2008) Studies on structure property relationship in a polymer–clay nanocomposite film based on $(PAN)_8LiClO_4$. J Polym Sci Part B Polym Phys 46:2577–2592
41. Jinisha B, Anilkumar KM, Manoj M, Pradeep VS, Jayalekshmi S (2017) Development of a novel type of solid polymer electrolyte for solid state lithium battery applications based on lithium enriched poly (ethylene oxide)(PEO)/poly (vinyl pyrrolidone)(PVP) blend polymer. Electrochim Acta 235:210–222
42. Roy A, Dutta B, Bhattacharya S (2017) Ion dynamics in NaBF4 salt-complexed PVC–PEO blend polymer electrolytes: correlation between average ion hopping length and network structure. Ionics 23(12):3389–3399
43. Wu F, Feng T, Wu C, Bai Y, Ye L, Chen J (2010) Thermally stable hyperbranched polyether-based polymer electrolyte for lithium-ion batteries. J Phys D Appl Phys 43(3):035501
44. Holomb R, Xu W, Markusson H, Johansson P, Jacobsson P (2006) Vibrational spectroscopy and ab initio studies of lithium bis (oxalato) borate (LiBOB) in different solvents. J Phys Chem A 110(40):11467–11472
45. Chowdhury FI, Khandaker MU, Amin YM, Arof AK (2017) Effect of gamma radiation on the transport and structural properties of polyacrylonitrile-lithium bis (oxalato) borate films. Solid State Ionics 304:27–39
46. Sharma AL, Thakur AK (2011) Polymer matrix–clay interaction mediated mechanism of electrical transport in exfoliated and intercalated polymer nanocomposites. J Mater Sci 46:1916–1931
47. Scrosati B, Croce F, Persi L (2000) Impedance spectroscopy study of PEO-based nanocomposite polymer electrolytes. J Electrochem Soc 147(5):1718–1721
48. Rai A, Sharma AL, Thakur AK (2014) Evaluation of aluminium doped lanthanum ferrite based electrodes for supercapacitor design. Solid State Ionics 262:230–233
49. Baskaran R, Selvasekarapandian S, Kuwata N, Kawamura J, Hattori T (2006) ac impedance, DSC and FT-IR investigations on (x) PVAc–$(1-x)$ PVdF blends with $LiClO_4$. Mater Chem Phys 98:55–61
50. Chilaka N, Ghosh S (2014) Dielectric studies of poly (ethylene glycol)-polyurethane/poly (methylmethacrylate)/montmorillonite composite. Electrochim Acta 134:232–241
51. Kesavan K, Mathew CM, Subbu C, Rajendran S (2014) Transport and optical studies of PEO/PVP/$LiClO_4$ based polymer blend electrolytes. Int J ChemTech Res 6:1810–1812
52. Tominaga Y, Ohno H (2000) Lithium-ion conduction in linear-and network-type polymers of PEO/sulfonamide salt hybrid. Electrochim Acta 45:3081–3086
53. Dhatarwal P, Sengwa RJ (2017) Dielectric and electrical characterization of (PEO–PMMA)–$LiBF_4$–EC plasticized solid polymer electrolyte films. J Polym Res 24:135
54. Koduru HK, Marino L, Scarpelli F, Petrov AG, Marinov YG, Hadjichristov GB, Iliev MT, Scaramuzza N (2017) Structural and dielectric properties of $NaIO_4$-complexed PEO/PVP blended solid polymer electrolytes. Curr Appl Phys 17:1518–1531
55. Kumar KK, Ravi M, Pavani Y, Bhavani S, Sharma AK, Rao VN (2011) Investigations on the effect of complexation of NaF salt with polymer blend (PEO/PVP) electrolytes on ionic conductivity and optical energy band gaps. Phys B Condens Matter 406:1706–1712

56. Naveen Kumar P, Sasikala U, Sharma AK (2013) Investigations on conductivity and discharge profiles of novel (PEO + PEMA) polymer blend electrolyte. Int J Innov Res Sci Eng Technol 2:3575–3582
57. Ramamohan K, Umadevi C, Achari VB, Sharma AK (2013) Conductivity studies on (PVC/PEMA) solid polymer blend electrolyte films complexed with $NaIO_4$. Int J Plast Technol 17:139–148
58. Kesavan K, Mathew CM, Rajendran S, Ulaganathan M (2014) Preparation and characterization of novel solid polymer blend electrolytes based on poly (vinyl pyrrolidone) with various concentrations of lithium perchlorate. Mate Sci Eng B 184:26–33
59. Salman YA, Abdullah OG, Hanna RR, Aziz SB (2018) Conductivity and electrical properties of chitosan–methylcellulose blend biopolymer electrolyte incorporated with lithium tetrafluoroborate. Int J Electrochem Sci 13:3185–3199
60. Khiar AA, Arof AK (2010) Conductivity studies of starch-based polymer electrolytes. Ionics 16:123–129
61. Ibrahim S, Yassin MM, Ahmad R, Johan MR (2011) Effects of various $LiPF_6$ salt concentrations on PEO-based solid polymer electrolytes. Ionics 17:399–405
62. Arya A, Sharma AL (2018) Enhancement in dielectric properties of blend solid polymer electrolyte with variation of temp and salt concentration. Macromol Res. https://doi.org/10.1007/s13233-019-7001-8
63. Arya A, Sharma AL (2018) Effect of salt concentration on dielectric properties of Li-ion conducting blend polymer electrolytes. J Mater Sci Mater Electron 29(20):17903–17920
64. Sharma AL, Thakur AK (2013) Plastic separators with improved properties for portable power device applications. Ionics 19(5):795–809
65. Sharma AL, Thakur AK (2010) Improvement in voltage, thermal, mechanical stability and ion transport properties in polymer-clay nanocomposites. J Appl Polym Sci 118(5):2743–2753
66. Kato Y, Watanabe M, Sanui K, Ogata N (1990) Ionic transport number of network PEO electrolytes. Solid State Ionics 40:632–636
67. Arya A, Nilesh Saykar G, Sharma AL (2018) Impact of shape (Nanofiller vs. Nanorod) of TiO_2 nanoparticle on free standing solid polymeric separator for energy storage/conversion devices. J Appl Polym Sci. https://doi.org/10.1002/app.20182193